Molecular Therapy
Methods & Clinical Development
Original Article

Getting the Most: Enhancing Efficacy by Promoting Erythropoiesis and Thrombopoiesis after Gene Therapy in Mice with Hurler Syndrome

Jing-fen Han,[1] Salim S. El-Amouri,[1] Mei Dai,[1] Phuong Cao,[2] and Dao Pan[1,2]

[1]Molecular and Cell Therapy Program, Division of Experimental Hematology and Cancer Biology, Cincinnati Children's Hospital Medical Center, Cincinnati, OH 45229, USA; [2]Department of Pediatrics, University of Cincinnati School of Medicine, Cincinnati, OH 45219, USA

Novel strategies are needed to solve the conundrum of achieving clinical efficacy with high vector copy numbers (VCNs) in hematopoietic stem cells (HSCs) while attempting to minimize the potential risk of oncogenesis in lentiviral vector (LV)-mediated gene therapy clinical trials. We previously reported the benefits of reprogramming erythroid-megakaryocytic (EMK) cells for high-level lysosomal enzyme production with less risk of activating oncogenes in HSCs. Herein, using a murine model of mucopolysaccharidosis type I (MPS I) with a deficiency of α-L-iduronidase (IDUA), we sought to determine the transgene minimum effective doses (MEDs) in major organs, and if a transient increase of IDUA-containing red blood cells and platelets by repeated phlebotomy would provide further therapeutic benefits in diseased mice after EMK-restricted LV-mediated gene therapy. The MEDs for complete metabolic correction ranged from 0.1 to 2 VCNs in major visceral organs, which were dramatically reduced to 0.005–0.1 VCN by one cycle of stress induction and were associated with a further reduction of pathological deficits in mice with 0.005 VCN. This work provides a proof of concept that transiently stimulating erythropoiesis and thrombopoiesis can further improve therapeutic benefits in HSC-mediated gene therapy for MPS I, a repeatable and reversible approach to enhance clinical efficacy in the treatment of lysosomal storage diseases.

INTRODUCTION

Lysosomal storage diseases (LSDs) are a group of inherited metabolic disorders, with a cumulative frequency of 1 in 5,000–7,000 live births that results from deficient activity in enzymes degrading various macromolecules within lysosomes of all cells.[1,2] Mucopolysaccharidosis type I (MPS I), or Hurler syndrome in its severe form, is caused by a deficiency of α-L-iduronidase (IDUA) (EC 3.2.1.76) and an accumulation of glycosaminoglycans (GAGs).[3,4] Gene therapy with lentiviral vector (LV)-mediated hematopoietic stem cell (HSC) gene transfer via autologous transplantation has demonstrated promising therapeutic benefits by overexpressing the correct version of lysosomal enzyme without the morbidity and mortality of allogeneic transplantation.[5–7] In fact, a recent HSC gene therapy clinical study for metachromatic leukodystrophy (a neurological LSD) has shown a clear halt of brain disease progression in patients with vector copy number (VCN) in various cell populations, ranging from 2.5 to 4.4 VCNs/genome,[8,9] suggesting a high transgene dose is essential to achieve clinical efficacy in LSD treatment. However, multiple independent integrations of the vector in every HSC genome also increase the potential risk of insertional mutagenesis,[10] which has become one of the major concerns in clinical application of gene therapy.[11–14] Novel strategies are needed to break the conundrum of high VCNs in HSCs that are required for achieving clinical efficacy but also present a higher, undesirable chance of oncogenesis in all offspring of transduced HSCs.

Red blood cells (RBCs) are the most abundant subset of blood cells with robust protein generation machinery. Platelets, the second most abundant subset with the shortest turnover time, are secretory particulate entities containing proteins stored and protected in cytoplasmic granules that can be released upon activation at a daily rate of 1%–5% in a healthy adult.[15–17] Importantly, both RBCs and platelets are enucleated cells, which is arguably one of the most effective safeguards against insertion-associated genotoxicity. Maintaining proper post-translational modifications for appropriate lysosomal trafficking and intercellular lysosomal enzyme transfer is essential for metabolic cross-correction in treating LSDs with multi-organ deficiencies.[7,18] We have recently shown that either maturing RBCs and/or megakaryocytes (MKs) are capable of producing large amounts of IDUA with proper catalytic function, lysosomal trafficking, and receptor-mediated uptake, which could be sorted to and stored within RBCs and platelets.[19,20] Moreover, supraphysiological levels of IDUA were achieved in the circulation of MPS I mice with only a moderate transgene dose (0.3 copy per HSC genome) when utilizing both lineages for IDUA expression, leading to complete correction in all peripheral organs tested. Significant reductions in brain pathology and behavioral deficits were also observed. A better understanding of dose

Received 1 August 2018; accepted 4 October 2018;
https://doi.org/10.1016/j.omtm.2018.10.001.

Correspondence: Dao Pan, PhD, Molecular and Cell Therapy Program, Division of Experimental Hematology and Cancer Biology, Cincinnati Children's Hospital Medical Center, 3333 Burnet Ave., Cincinnati, OH 45229, USA.
E-mail: dao.pan@cchmc.org

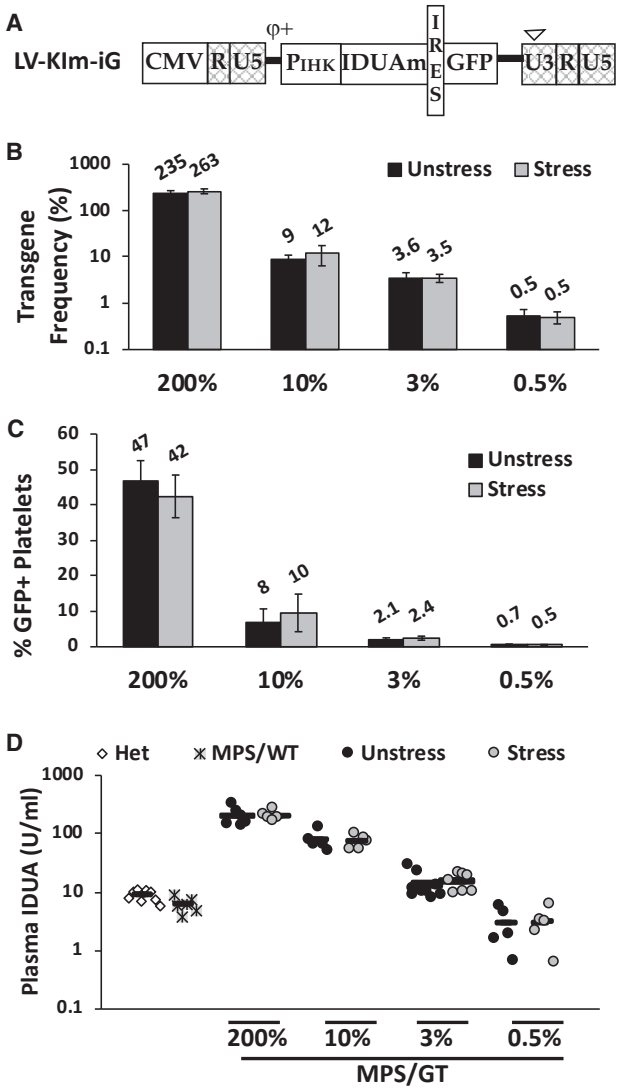

Figure 1. Long-Term Expression of Transgenes and Gene Transfer Efficiency in MPS I Chimeras with Various Gene Doses when Utilizing Lineage-Restricted LV

MPS I mice (8–10 weeks old) were transplanted with either WT bone marrow (MPS/WT) or LV-transduced Lin$^-$ MPS I cells (transduced at an MOI of 40 and resulted in ~45% GFP$^+$ platelets 4 months after BMT). Secondary transplantation was conducted to generate various transgene-dose groups (including 200%-undiluted, 10%, 3%, and <1%) using a serial dilution of bone marrow from primary recipients (2.2–2.6 VCNs) with those from untreated MPS I mice. A subset of mice from each dose group (Stress) was given stress-phlebotomy (350–400 μL) via retro-orbital vein in 2 consecutive days. (A) Illustration of lentiviral vector construct. P_{IHK}, erythroid and MK-restricted hybrid promoter; IDUAm, human *IDUA* cDNA in-frame fused at 3′ with myc tag; IRES, internal ribosome entry site. (B) Transgene frequencies in each dose group with or without stress. RT-qPCR was conducted using low-density bone marrow cells isolated from mice ~6 months after BMT. (C) Percentages of GFP-containing platelets 5 months after transplantation. Whole blood was collected before stress-phlebotomy, followed by immunostaining with anti-CD41-PE and analyzed by FACS. (D) Plasma IDUA levels 5 months after transplantation (before stress-phlebotomy). Black bars represent mean of each group, and data were derived from 5–9 mice per group. Error bars, SD of 5–9 mice; Het, healthy heterozygous mice.

correlation of long-term HSC gene transfer at relatively low frequencies (<20%) via RBC/MK lineages with visceral and CNS cross-correction would be critical for future therapeutic implications, and it is yet to be determined.

Approximately 85 clinical trials of HSC-mediated gene therapy have been conducted for monogenic diseases worldwide, utilizing onco-retroviral or lentiviral vectors (http://www.abedia.com/wiley/). Despite the significant progress made to increase transduction efficiency into successfully engrafted HSCs,[21] there is ample room to improve therapeutic efficacy. In addition, the frequencies of genetically corrected, successfully engrafted HSCs varied markedly among patients even within the same clinical trials,[8,22] and it may not be practical to repeat HSC-mediated gene therapy in the same patient.

The generation of both RBCs and platelets can be increased substantially in humans and other mammals during times of acute or chronic stress, such as acute trauma (blood loss) or hemolysis.[23] In addition, strategies of inducible growth of transgene-containing HSC or its offspring in specific lineages (RBCs and platelets) have been developed.[24–28] Herein we tested the hypothesis that a transient increase of IDUA-containing RBCs and platelets by stress erythropoiesis and thrombopoiesis would provide additional therapeutic benefits in MPS I mice after HSC gene therapy with lineage-restricted IDUA expression. After one cycle of repeated phlebotomy, plasma IDUA activity increased correspondingly to the elevated proliferation of RBCs, MKs, and platelets in MPS I, with various transgene doses (ranging from 0.005 to 2 VCNs/cell) derived from HSC-mediated gene therapy. A preclinical efficacy study was conducted to evaluate stress-induced IDUA redistribution, as well as its additional benefits in metabolic correction and normalization of lysosomal storage pathology. The results also defined the minimum effective dose (MED) for long-term phenotypic correction in peripheral organs, while the correlation of transgene doses with CNS phenotypic improvement has been reported previously in a similar setting.[29] This work provides a proof of concept that manipulating erythropoiesis and thrombopoiesis can further improve therapeutic benefits in HSC-mediated gene therapy of MPS I, a repeatable and reversible approach to enhance clinical efficacy of gene therapy.

RESULTS

Highly Efficient Release of IDUA in Circulation Was Detected with Gene-Dose Dependence when Restricting Transgene Expression in Erythroid and MK Lineages

It has been demonstrated previously that a hybrid promoter (IHK) could introduce supra-physiological levels of plasma IDUA (10- to 12-fold of normal carrier levels) after LV-mediated HSC gene transfer, with only 0.2–0.3 VCN/cell, by restricting transgene expression in erythroid-megakaryocytic (EMK) lineages.[20] In this study, IHK promoter was utilized to co-express EGFP and a human IDUA protein with a myc-tag at the C terminus (Figure 1A). Primary MPS I chimeras (n = 3) were established by transplantation of diseased HSCs

that had been transduced with LV-KIm-iG at 40 multiplicity of infection (MOI), resulting in transgene frequencies of 2.2–2.6 VCNs/cell in bone marrow 4 months after transplantation. To generate various transgene-dose groups, bone marrow cells from primary MPS I chimeras were transplanted into secondary MPS I recipients directly (for the highest gene-dose group) or with serial dilution into marrow from MPS I mice (for low-gene-dose groups). At 5 months after transplantation, a subset of mice from each dose group was given stress phlebotomy (350–400 μL) via retro-orbital vein in 2 consecutive days, followed by organ harvest 6 weeks later.

At the end of the observation period (~7 months after bone marrow transplantation [BMT]), transgene frequency in secondary recipients was determined by real-time qPCR using total bone marrow (Figure 1B). Based on transgene frequency, the gene therapy-treated MPS I animals (MPS/GT) were divided into four gene-dose groups as 200% (mean of 235% for unstressed subgroup or 263% for stressed subgroup), 10% (mean of 9% or 12%), 3% (mean of 3.6% or 3.5%), and 0.5% (mean of 0.5% for both). To evaluate transgene expression, GFP-positive RBCs and platelets were determined by fluorescence-activated cell sorting (FACS) analysis 5 months after transplantation (Figure S1). Unlike RBCs for which GFP detection would be obscured by hemoglobin, the frequency of GFP^+ platelets, as gated by size and $CD41^+$ marker, showed a direct correlation with gene doses, except for the 200% MPS/GT group when multiple insertions are often predicted within transductants (Figure 1C).[30,31]

To determine IDUA release into the circulation during normal erythropoiesis and thrombopoiesis, baseline plasma IDUA activities were measured using blood samples with a normal base rate of platelet activation (<5% Annexin-V^+) prior to any stress phlebotomy (Figure 1D). Comparable levels of plasma IDUA were detected in both unstressed and stressed mice within each dose group. The mean plasma IDUA activity in the 200% MPS/GT group was 199 U/mL for both subgroups (equivalent to ~450 U/mL/GFP^+ cell but ~80 U/mL/copy based on qPCR data), which was 20-fold higher than that in normal heterozygous mice (mean of 9 U/mL). Among the three low-gene-dose groups, the mean IDUA activity levels in the 10% MPS/GT group (74 U/mL for unstressed and 72 U/mL for stress subgroups) were equivalent to ~820 or 720 U/mL/GFP^+ cell, respectively, while plasma IDUA levels in the 3% MPS/GT group (mean of 14 U/mL and 15 U/mL, respectively) were equivalent to ~670 or 630 U/mL/GFP^+ cell. The plasma IDUA levels in the 0.5% MPS/GT group (mean of 3 U/mL for both subgroups with a range of 0.6 to 6 U/mL) were equivalent to ~460 or 600 U/mL/GFP^+ cell. MPS I mice fully engrafted with wild-type bone marrow (MPS/WT) exhibited near-heterozygous plasma IDUA activities (mean of 6.5 U/mL) that were equivalent to 3.2 U/mL/endogenous IDUA copy. These data suggest that the transgene-derived plasma IDUA levels are directly correlated to both the frequency of GFP-expressing platelets and the transgene doses in BM at lower transgene-dose groups (≤10%), with up to ~200-fold more IDUA released into the circulation from lineage-restricted promoter than from endogenous IDUA promoter. Normalization of plasma IDUA was ascertained in MPS/GT mice with as low as 0.5% HSC transduction efficiency when utilizing erythroid, MK, and platelet lineages for lysosomal enzyme expression.

Erythropoiesis and Thrombopoiesis Induced by Repeated Phlebotomy Stress Were Associated with an Increase in IDUA Released into the Circulation

With a lifespan of 120 days for RBCs or 9–10 days for platelets, an adult human must maintain a baseline daily production rate of ~1% for RBCs and 10% for platelets under steady-state conditions.[32] These levels of production can be increased greatly under conditions of increased demand (i.e., stress), such as acute trauma or blood loss.[33,34] To evaluate if transgene-derived IDUA expression and release can be further enhanced after stress, we performed large-volume (350- to 400-μL) bleeding on 2 consecutive days, followed by small-volume blood sampling in a subset of animals from each dose group and controls (Figure S2A).

A transient reduction of hematocrit and RBC counts occurred right after the first retro-orbital bleeding on day 2 and reached a nadir around day 4, followed by gradual recovery toward baseline levels on day 10 for hematocrit and day 23 for RBC counts in normal controls, with a much slower recovery observed in transplantation recipients (Figure S2B and S2C). Importantly, erythropoiesis induced by stress was verified with up to a 5-fold increase in the percentages of reticulocytes on day 7, by FACS analysis with Thiazole Orange staining, and it was followed by a gradual return to the normal levels on day 30 (Figure 2A; Figure S3A). Reactive thrombocytosis was observed with a more rapid increase of young platelets when staining with CD41-PE and Thiazole Orange (for RNA), which peaked from 8.6%–9.2% to 20%–23% on day 4 and returned to baseline on day 16 (Figure 2B; Figure S3B). This increase in platelet formation was also reflected by changes in platelet counts (Figure S2D). Moreover, plasma IDUA activities were elevated significantly on day 7 (associated with peaks of reticulocyte production) in all but the 0.5% MPS/GT group, with increases that were 4.5-, 2-, and 1.5-fold above baseline levels in the 200%, 10%, and 3% groups, respectively, and they returned to baselines by day 23 (Figure 2B). These data demonstrated that significant but temporary elevation of plasma IDUA could be achieved by stress erythropoiesis and thrombopoiesis reactive to blood loss in MPS/GT mice, with gene transfer efficiency of more than 3% when utilizing erythroid and MK lineages for transgene expression.

Different Organs in MPS/GT Mice Exhibited Various Levels of Functional IDUA Enzyme in Response to Stress Phlebotomy

To better understand dose correlation and the effect of stress erythropoiesis and/or thrombopoiesis on organ distribution of the IDUA enzyme, we assessed IDUA activities in major affected organs from animals after transcardiac perfusion at ≤9 months of age (i.e., ~6 weeks after phlebotomy) (Figure 3). Among unstressed MPS/GT mice, the highest gene-dose group exhibited higher-than-normal IDUA levels in the spleen (3.6-fold) and liver (2.5-fold), with only

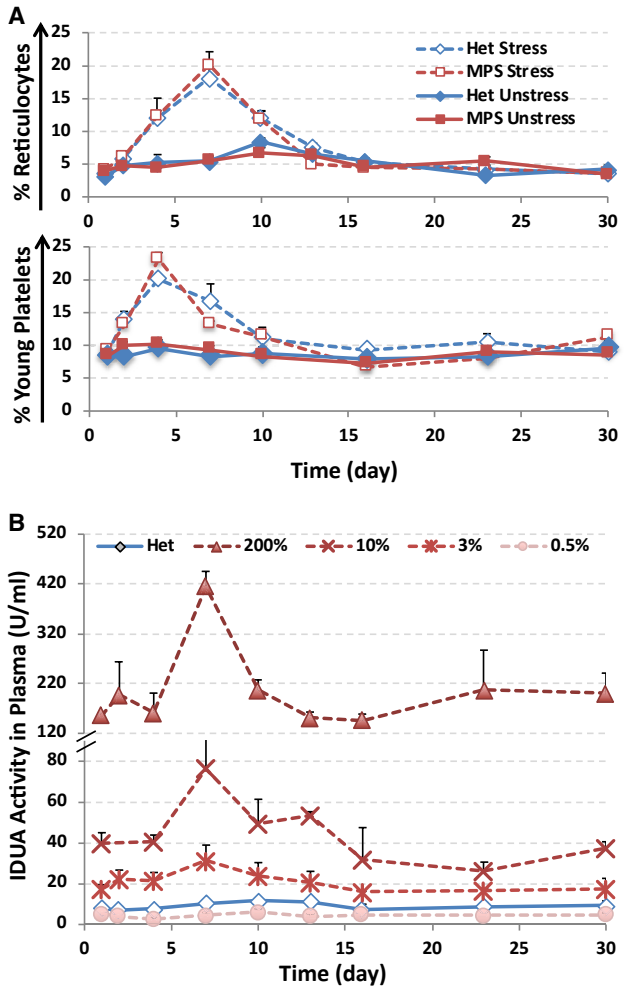

Figure 2. Stress Erythropoiesis and Thrombopoiesis in Response to Repeated Phlebotomy Led to an Increase in Plasma IDUA

(A) Changes in the percentages of reticulocytes (top) or RNA-containing young platelets (bottom) as determined by FACS analysis with Thiazole Orange and CD41-PE staining. Data are presented as mean ± SD (n = 6–15) (error bars). (B) Plasma IDUA activities among various gene therapy groups after stress phlebotomy. Data were derived from 5–9 mice per group, and error bars represent SD.

partially normalized enzyme levels found in the kidney (21%) and the heart (12%). Compared to MPS I mice fully engrafted with wild-type HSCs (MPS/WT), the 200% MPS/GT group presented significantly higher tissue IDUA levels in the liver (6-fold), spleen (4-fold), kidney (2.3-fold), and heart (1.8-fold). A gene-dose correlation was observed with IDUA activities in the spleen, liver, and kidney of various MPS/GT groups, although barely detectable IDUA levels were obtained in the heart of all low-dose MPS/GT groups. These results demonstrated different organ distribution capabilities of erythroid- and MK-derived IDUA in treated MPS I mice, i.e., 82% of transgene-derived IDUA found in the spleen > 15% in liver > 1.5% in kidney > 0.5% in heart, in comparison to those in mice with conventional BMT treatment (spleen > liver > kidney = heart).

Importantly, in comparison to unstressed MPS/GT mice, elevated IDUA levels were found in the spleen and liver among all dose groups (2.5- to 4.1-fold) (except for the liver of MPS/GT 200%) 6 weeks after the introduction of stress phlebotomy, resulting in the normalization of spleen enzyme activity in MPS/GT 10% mice. The IDUA activity in the kidney was apparently responsive to stress, with an increase in MPS/GT 10% and 3% groups. In the heart, the most responsive gene-dose group was MPS/GT 10% with significant enhancement from hardly detectable levels in unstressed mice to those comparable to MPS/WT. The data suggested that the minimal transgene dose for detectable organ IDUA was 0.5% for spleen and liver, with $\geq$3% for kidney and $\geq$10% for heart. In addition, the spleen and liver were the most responsive organs to stress phlebotomy, followed by the heart and kidney.

Long-Term Biodistribution of IDUA in Affected Organs

To identify the cell types targeted for delivery of full-length IDUA derived from erythroid and megakaryocyte lineages, we evaluated the affected visceral organs from well-perfused MPS/GT mice, by immunofluorescence analysis using anti-myc antibody for the myc tag fused at the C terminus of IDUA (Figure 4). In the spleen of unstressed MPS/GT mice (3% gene-dose group as an example), myc-positive signals were mostly detected in endothelial cells of blood vessels and red pulps, as indicated by co-localization with TER119$^+$ (an erythroid marker), as well as in CD41$^+$ MK cells (Figure 4A). After stress phlebotomy, a similar pattern was observed in red pulps but with a more intensified distribution than that of the same dose group without stress. CD41$^+$ MK cells became relatively abundant, many of which were associated with myc$^+$ (IDUA), in comparison to those in unstressed mice.

In the liver, the relatively abundant, abnormally large CD68$^+$ cells (most likely Kupffer cells) found in untreated MPS I mice were dramatically reduced by both the number and size in MPS/GT mice, with as low as 0.5% GT (Figure 4B). The sparse distribution of IDUA myc$^+$ signals found in cubic hepatocytes of MPS/GT 0.5% mice became more visible and often centered around blood vessels with increased gene doses (3% and 10%). After stress induction, myc$^+$ signals in the lowest dose group were more intense, although still relatively sparse, in patches of hepatocytes. Strong IDUA myc$^+$ signals were observed throughout the liver of stressed mice in the 10% MPS/GT group.

In the kidney of MPS/GT mice, myc$^+$ signals were not always co-localized with CD68$^+$ cells regardless of stress conditions, although the numbers and aggregates of these CD68$^+$ tissue macrophages appeared to be reduced to normal levels in MPS GT-treated mice (Figure 4C). The myc$^+$ staining was mainly detected in tubular epithelial cells that were positive for E-cadherin staining. Interestingly, strong IDUA myc$^+$ signals were also detected in the glomerulus after stress phlebotomy, with as low as 10% transgene frequency. These results

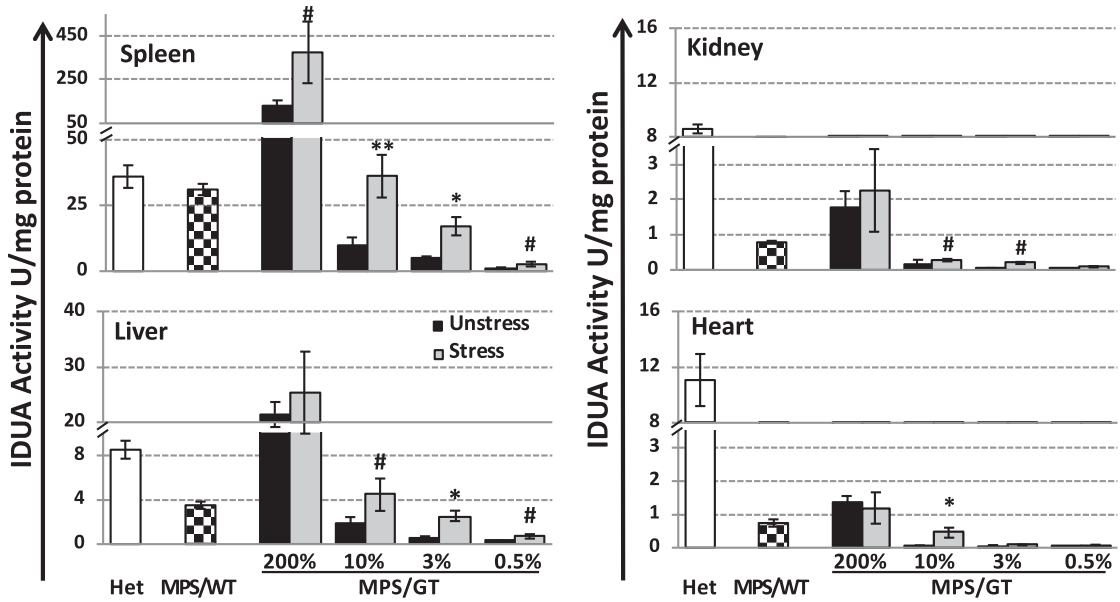

Figure 3. IDUA Enzymatic Activity in Peripheral Organs from Perfused Animals with or without Stress Phlebotomy

Organs were harvested from perfused animals 6 weeks after repeated phlebotomy (i.e., at ~9 months of age) and tested for IDUA activity in triplicate. An undetectable level of IDUA activity (<0.005 U/mg) was found in organs of MPS I mice regardless of stress phlebotomy. Data were derived from 5–7 animals per group with error bars representing the SEM. $^{**}p \leq 0.01$, $^{*}p \leq 0.05$, and #$0.05 < p < 0.1$ by the Student's t test when comparing between stressed and unstressed mice of the same dose group.

documented the diverse distribution of erythroid and MK-derived IDUA and the differences in cell types that benefited from stress induction among affected organs.

Synergistic Effect of Stress Erythropoiesis and Thrombopoiesis Resulted in a Further Reduction of Organ GAG Accumulation

To evaluate the threshold transgene levels for systemic metabolic correction and the potential of therapeutic benefits by stress erythropoiesis and thrombopoiesis, we assessed GAG levels in the urine of treated MPS I mice in comparison with age-matched untreated MPS I and normal mice before and after repeated phlebotomy (Figures 5A and 5B). The reduction of urinary GAG accumulation was inversely correlated to transgene doses, with significant improvement found at the dose of ≥3% 5 months after transplantation. No significant difference was observed in urine GAG levels between normal and treated MPS/GT groups with ≥10% transgene frequency ($p = 0.185$ when comparing 10% MPS/GT with Het groups), suggesting a threshold transgene dose (10%) for systemic metabolic correction in MPS I mice. Importantly, when subjected to stress induction, both the 3% and 0.5% MPS/GT groups exhibited significant GAG reduction in urine from their baseline levels around day 7, which stayed relatively low until the end of the observation period (day 30). The data implicated an additional systemic metabolic improvement (i.e., urinary GAG reduction) resulted from stress phlebotomy.

To determine the response of metabolic accumulation to stress bleeding and therapeutic threshold in affected organs, we quantified GAG levels ~7 months post-transplantation in the brain, spleen, liver, kidney, and heart (Figures 5C and 5D). Brain GAG levels reduced significantly in GT-treated mice with over 3% efficiencies, and they did not normalize in the highest dose group (200% GT), which is consistent with previous observations in similar experimental settings.[29] Comparable levels of brain GAGs were detected between unstressed and stressed mice within all gene-dose groups (data not shown). Without stress bleeding, complete normalization of GAGs was observed in all peripheral organs tested at the highest dose group (MPS/GT 200%) and in MPS/WT treatment controls. The reduction of organ GAG levels was inversely associated with the increase of transgene doses by various thresholds for significant benefits in spleen (≥0.5% transgene frequency), liver (≥0.5%), and kidney (≥10%). In the heart, as low as 0.5% GT was sufficient to introduce significant GAG reduction compared to untreated MPS I mice, but similar levels were found in all but the highest MPS/GT dose groups.

Importantly, upon stress phlebotomy, spleen GAG levels significantly decreased even further in all low GT groups, reaching normalization with the lowest transgene dose (0.5%). Metabolic correction was achieved in the liver of 10% and 3% MPS/GT groups after one cycle of stress bleeding, although similar levels were observed in the lowest dose group. No significant difference was found in the kidney or the heart of most MPS/GT dose groups with or without stress bleeding, except for the heart at the 10% GT dose. These results demonstrated that complete metabolic correction could be achieved by stress induction in the spleen at the lowest dose tested (0.5%), in the liver at 3%, in

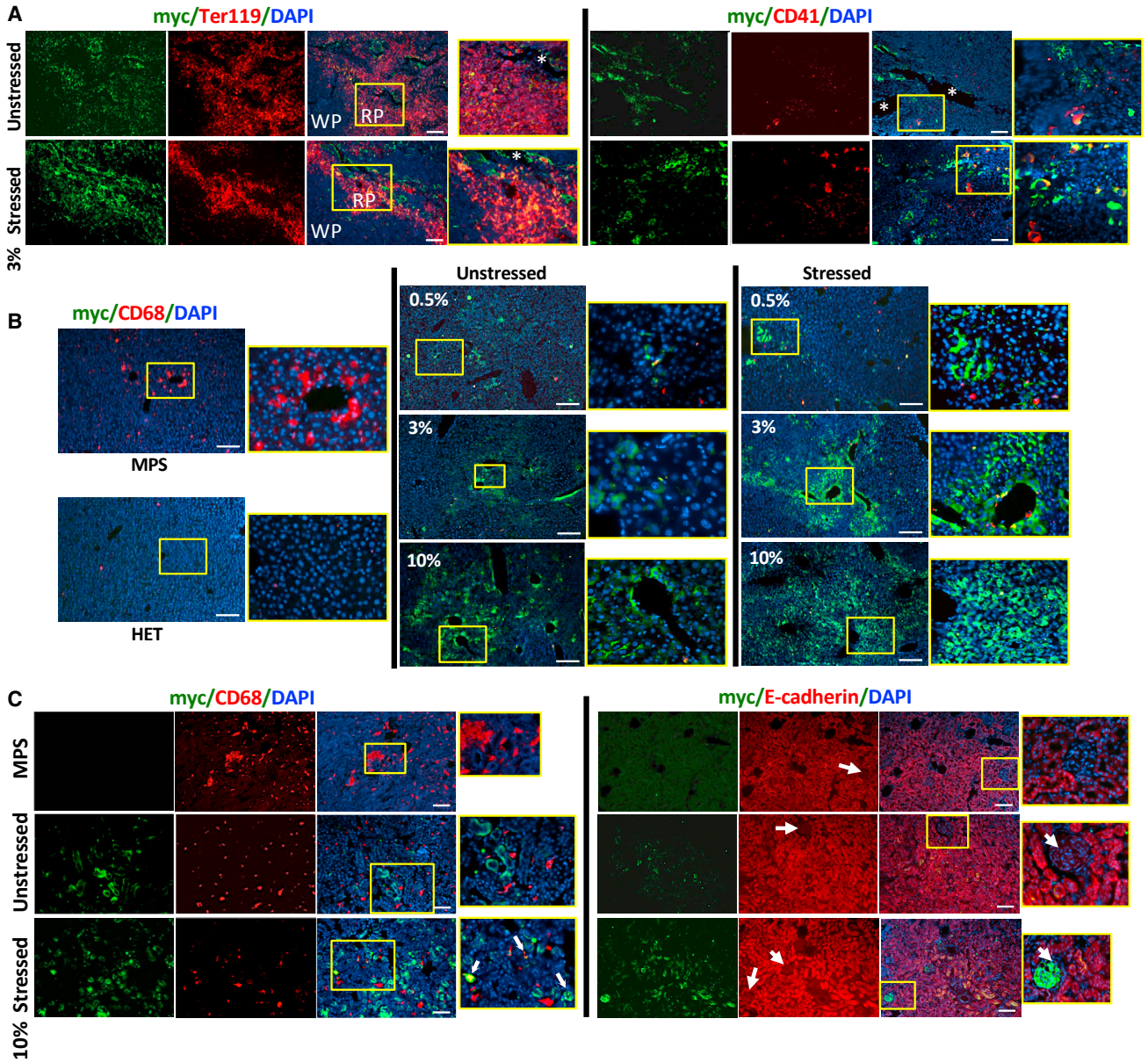

Figure 4. Immunofluorescence Analysis for the Biodistribution of Full-Length IDUA in Spleen, Liver, and Kidney

Frozen tissue sections were obtained from perfused animals ~7 months after HSC-mediated gene therapy using erythroid and MK-restricted LV, with or without the induction of stress phlebotomy. (A) Representative images of spleen sections from 3% MPS/GT groups. Samples were stained with antibodies against myc tag (green) for full-length IDUA, TER119 (red, left panel) for erythroid cells, or CD41 for megakaryocytes/platelets, and they were counterstained with DAPI (blue) for nuclei. *blood vessels; WP, white pulp; RP, red pulp. (B) Representative images of liver sections from perfused mice of different MPS/GT dose groups. Samples were stained with antibodies against myc tag (green) for IDUA or CD68 (red) for Kupffer cells, and they were counterstained with DAPI (blue) for nuclei. (C) Representative images of kidney cortex sections from stressed or unstressed mice in the 10% MPS/GT group. Samples were stained with antibodies against myc tag (green) for full-length IDUA, CD68 (red, left panel) for resident macrophages, or E-cadherin (CDH1) (red, right panel) for tubular epithelial cells, and they were counterstained with DAPI (blue) for nuclei. Arrow, kidney glomeruli. Scale bars, 100 μm for all images. Areas within yellow boxes are amplified and showed on the right of each view.

the heart at 10%, and in the kidney at the highest dose. The data also suggested that stress erythropoiesis and thrombopoiesis could provide significant therapeutic advantages for GAG reductions in the spleen, liver, and heart, with different MEDs, and no response in the kidney.

Threshold Gene Dose for Pathology Improvement Varied among Organs with Further Therapeutic Advantages Empowered by Stress Bleeding

To determine threshold doses for pathology improvement by erythroid and MK-restricted IDUA expression and evaluate therapeutic response

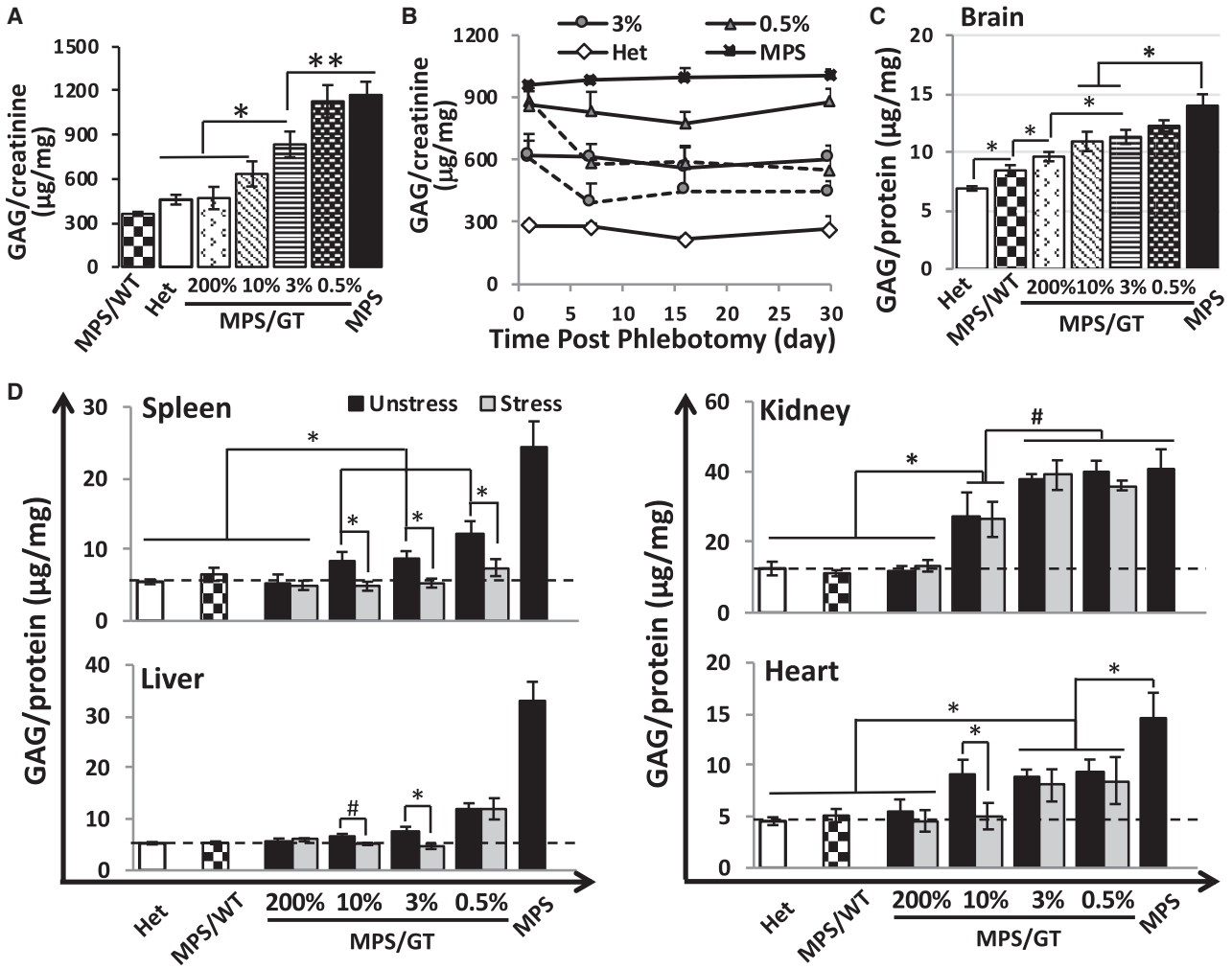

Figure 5. Dose-Responsive, Stress-Sensitive, and Organ-Divergent Metabolic Correction in Gene Therapy-Treated MPS I Mice

(A) Urinary GAG levels were determined by the GAG-DMMB (1,9-dimethylmethylene blue) decomposition assay 5 months after transplantation before stress-phlebotomy. (B) Change of GAG levels in urine after stress phlebotomy. Dotted lines represent stressed groups and solid lines are for unstressed controls (n = 4–6 for all groups). Note, no significant difference was observed between normal heterozygous levels and MPS/GT 200% ($p = 0.911$) or 10% ($p = 0.185$). (C) GAG levels in the brains of unstressed mice. Two pieces of forebrain cortex were tested for each animal. Note, similar levels of brain GAGs were detected regardless of being stressed or not within the same gene-dose group (data not shown). (D) GAG accumulation in peripheral organs. Dotted lines indicate GAG levels in normal heterozygote mice. $^{**}p < 0.01$, $^{*}0.01 < p < 0.05$, and #$0.05 < p < 0.1$ by Student's t test; n = 5–9 for all dose groups in organ GAG analyses; error bars represent SEM for all. GAG levels were normalized by either creatinine (for urine samples) or protein (for tissues) levels.

to one treatment cycle of stress phlebotomy, we performed histopathology analysis in the affected peripheral organs of MPS/GT mice ~6 weeks after stress induction. In the spleen, characteristic storage vacuoles observed in perisinusoidal cells of red pulps in untreated MPS I mice were fully corrected in MPS/GT mice with the lowest dose group (0.5%), regardless of stress bleeding (Figure S4).

In the liver, the percentage of distended Kupffer cells with massive vacuoles was significantly reduced from 57% in untreated MPS I to 21% in the lowest dose group of MPS/GT, which was completely normalized in the stressed mice of the same dose group (Figures 6A and 6B). A considerable reduction of vacuolated hepatocytes was also observed in the lowest dose group, with a significantly further improvement by stress in both the 0.5% and 3% dose groups. Complete pathological correction was detected in Kupffer cells by 3% GT and in hepatocytes by 10% GT (data not shown) of unstressed MPS/GT mice.

Diseased kidneys exhibited pathological vacuoles in interstitial cells, which were completely normalized in the highest gene-dose group but were indistinguishable from any of the lower dose groups (Figures 6C and 6D). Importantly, stress phlebotomy introduced significant and dose-correlated improvement of kidney pathology in MPS/GT mice with 3% and 10% transgene frequency.

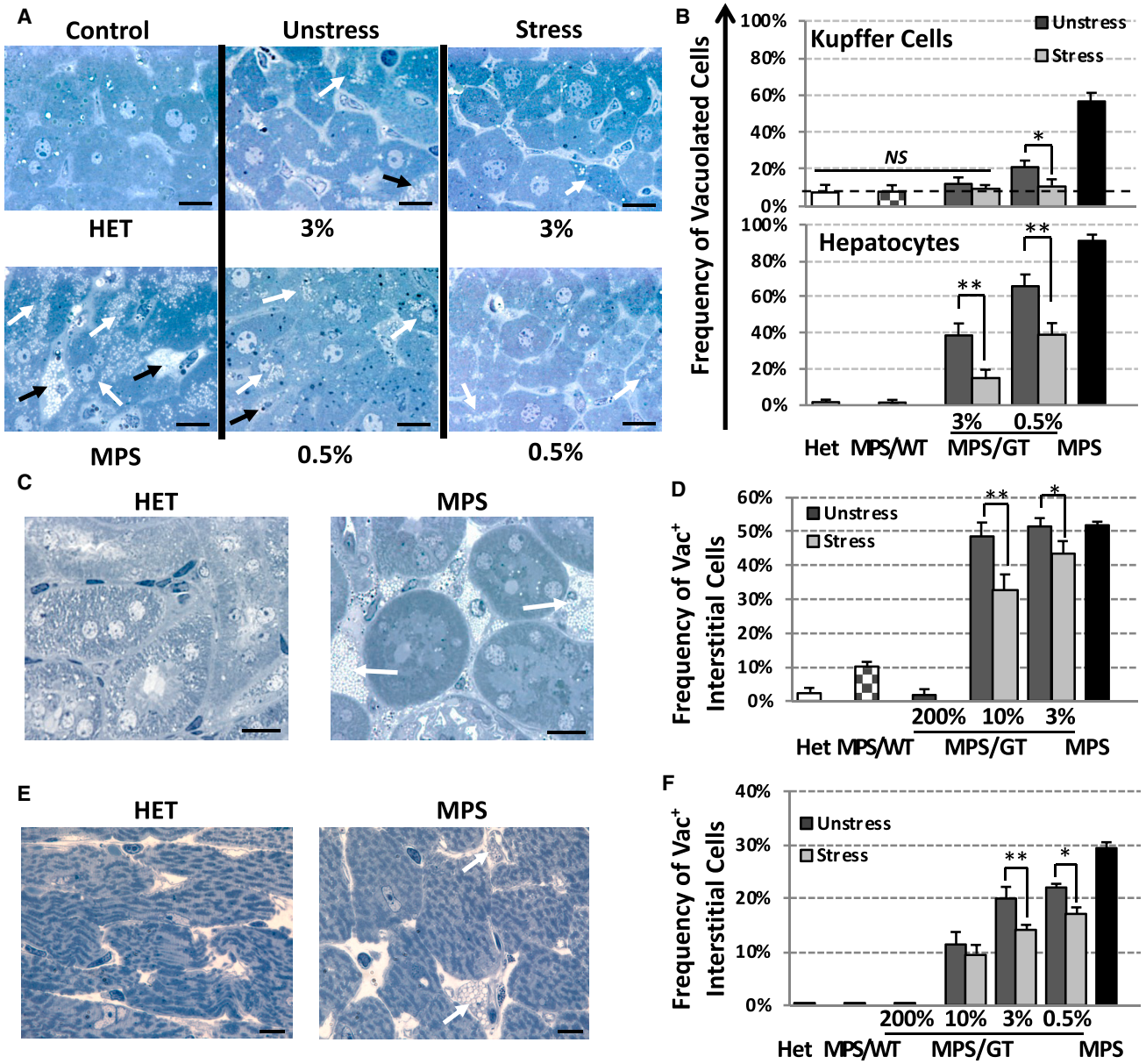

Figure 6. Improvement of Pathology in Peripheral Organs by Stress Erythropoiesis and Thrombopoiesis within Different Dose Groups

Histopathology analysis of liver (A and B), kidney (C and D), and heart (E and F) was conducted in Epon-embedded semithin sections (0.5–1 μm) with toluidine blue staining. (A) Representative views of liver sections showing normal (in heterozygote mouse, HET) or abnormal hepatocytes (white arrows) and Kupffer cells (black arrows) with massive storage vacuoles in untreated or some treated MPS I mice. Scale bars, 20 μm. (B) Percentage of Kupffer cells and hepatocytes that are associated with large amounts of vacuoles (≥15 vacuoles for hepatocytes and ≥5 for Kupffer cells). Note, normalized pathology was observed in livers of MPS/GT at higher dose groups (i.e., 10% and 200% groups). (C) Representative views of kidney sections showing interstitial cells with (white arrows) or without storage vacuoles. Scale bars, 50 μm. (D) Frequency of interstitial cells that are distended and associated with massive vacuoles. (E) Representative views showing cells with or without storage inclusions (white arrows) in interstitial tissues of hearts with storage vacuoles. Scale bars, 20 μm. (F) Percentage of vacuolated cells. The scoring data were derived from ≥6 sections of 2–4 slides of 1–3 mice per group, and error bars represent the SEM. **$p < 0.01$ and *$0.01 < p < 0.05$ by Student's t test.

Consistent with observations reported by others,[35,36] storage inclusions were present in cells (mostly macrophages) within interstitial tissues of the heart in untreated MPS I mice (Figures 6E and 6F). Significant improvement was already observed in the lowest dose group, with further benefits achieved by one cycle of stress phlebotomy in the 0.5% and 3% MPS/GT groups, but not in 10% MPS/GT mice.

These observations demonstrated that the gene dose required for pathological correction varied among organs, with the lowest requirement for the spleen (0.5%) and followed by the liver (3% or 10%), heart (200%), and kidney (200%), when utilizing maturing RBCs, MKs, and platelets as expression and delivery vehicles. The data also suggested that further therapeutic benefits could be achieved by stress phlebotomy, with as low as 0.5% GT for the liver and heart and 3% GT for the kidney.

DISCUSSION

The research described here not only represents a comprehensive preclinical evaluation of an HSC-mediated gene therapy approach when utilizing erythroid and MK lineages for transgene overexpression, delivery, and distribution in a murine model of LSD (i.e., Hurler syndrome), but also documents the feasibility of improving therapeutic efficacy by transiently promoting erythropoiesis and thrombopoiesis. The minimum effective transgene dose for metabolic normalization (GAGs) was determined for major visceral organs, including the liver (0.1 VCN), spleen (1 VCN), heart (2 VCNs), and kidney (2 VCNs). Such efficacy can be ultimately achieved with dramatically reduced gene doses after one cycle of transient elevation of RBC and platelet production, with the spleen as the organ that benefits the most (from 1 to 0.005 VCN), followed by the heart (from 2 to 0.1) and liver (from 0.1 to 0.03), with no change for the kidney. Tissue pathology presented as vacuolated interstitial cells was completely corrected in the spleen of the lowest dose group (0.005 VCN), in the liver with 0.03 VCN, and in the heart and kidney with 2 VCNs. Significant improvement of tissue pathology after stress phlebotomy was observed with as low as 0.005 VCN in the liver and heart and with 0.03 VCN in the kidney. These results highlighted robust efficacy when using erythroid and MK lineages for overexpression of a lysosomal enzyme. The further reduction of MEDs for complete metabolic correction and pathological improvement in visceral organs of MPS I mice in response to one cycle of stress phlebotomy documents the high efficacious potential of stimulating erythropoiesis and thrombopoiesis to further boost therapeutic benefits of gene therapy in MPS I patients.

HSC-mediated gene therapy with gamma-retroviral vectors (RVs) or LVs has been successfully applied in clinical trials for the correction of Wiskott-Aldrich syndrome (WAS),[37,38] X-linked severe combined immunodeficiency (X-SCID),[39] Sickle cell disease,[40] X-linked adrenoleukodystrophy,[41] and metachromatic leukodystrophy.[8,9] The leukemia cases are all associated with RV-transduced, enhancer-mediated (proto)-oncogene activation.[14] Replacing strong viral enhancers and promoters with housekeeping gene promoters in SIN-RV or LV seems to reduce catastrophic genetic events. However, therapeutic efficacy in LSD treatment has been highly correlated with enzyme doses achieved in animal models[29,42] or clinical experience, including gene therapy clinical trials and HSC transplantation with the choice of donors (healthy versus carriers).[8,43] To compensate for utilizing relatively weak cellular promoters (such as the *PGK* promoter), above-normal enzyme levels needed for significant clinical efficacy would require multiple proviral insertions in each HSC that present a higher risk of oncogenesis in all offspring of transduced HSCs.[6] We have shown here that up to ~200-fold more IDUA is released into the circulation when IDUA expression is driven by an erythroid and MK lineage-restricted hybrid promoter compared to an endogenous IDUA promoter. Importantly, systemic metabolic correction shown by urine GAG normalization was achieved in mice with as low as 0.1 VCN and above-normal plasma IDUA (~8-fold of normal heterozygous), with significant GAG reduction observed in the brain and complete pathological correction in the liver and spleen. The CNS benefits detected here are consistent with the observations by us in a similar LV setting[29] or by others that repeated, high-dose enzyme replacement therapy (ERT)-facilitated IDUA transit across the blood-brain barrier (BBB), resulting in the reduction of brain GAG accumulation and improvement in cognitive deficits.[44] Besides being boosted by efficient protein generation by exploiting the enormous cell mass and relatively quick turnover of RBCs and platelets, therapeutic efficacies are maximized by versatile enzyme transport and on-target protein delivery. The enzyme released in the bloodstream will be taken up via M6P receptor-mediated endocytosis or transcytosis or pinocytosis by other cells, such as endothelial cells, monocytes and/or macrophages, and other blood cells. Moreover, the clearance of senile platelets is mediated by the mononuclear phagocyte system that primarily resides in the spleen and lymph nodes, as well as Kupffer cells and hepatocytes of the liver.[45] Our data have shown widespread IDUA-containing $CD68^+$ macrophages or interstitial cells, the most affected sites in many LSDs, in all organs tested. These observations highlight the advantage of utilizing and/or including the MEK lineage for highly efficient systemic protein production and release and on-target distribution into monocytes and/or macrophages with robust therapeutic benefits.

In addition to high enzyme doses achieved in circulation, sufficient levels of enzyme attained within proper cell types and organs have also been proven valuable for advanced efficacy in this and other preclinical models.[46] Tissue macrophages are one of the main effector cells in many LSDs, and they are associated with more prominent and rapid substrate accumulation.[47] Apparently, a small fraction of normal heterozygous IDUA levels in the heart (12%) or kidney (20%) was sufficient to normalize completely both the organ GAGs and pathologic abnormalities shown as vacuolated interstitial cells (mostly macrophages), suggesting tissue macrophages as the main contributor to the elevation of GAGs in the heart and kidney. Interestingly, the clearance of abnormal Kupffer cells in the liver would entail as low as 7% of normal enzyme levels, but up to 22% of normal enzyme levels is required for complete correction of liver substrate accumulation and hepatic pathology. The preferential distribution of IDUA to the mononuclear phagocyte system provided by platelet and/or RBC-mediated delivery may be accredited to the lower demand of IDUA enzyme for Kupffer cell normalization. In the spleen, complete pathologic normalization (vacuolated cells) was achieved with minimal levels of IDUA (3% of normal) found in the lowest treated group, which coincided with the fact that the spleen obtained the highest enzyme levels among all organs tested when delivering via erythroid and MK lineages. However, it takes much more enzyme

(>30% of normal) to obtain spleen GAG normalization. This is likely due to the relatively less IDUA distribution, compared to red pulps and marginal zones, in white pulps, which also seem to play a considerable role in GAG accumulation in the spleen.

The one-cycle, stress-induced erythropoiesis and thrombopoiesis lead to preferential therapeutic benefits among various organs. The spleen is the most responsive organ that showed a significant increase in tissue IDUA and a reduction of GAGs, with as low as 0.005 VCN. This is largely attributable to the facts that one-third of platelets are pooled in the spleen as a reserve, released when needed by sympathetically induced splenic muscle contractions,[48] and that the spleen contains a unique microenvironment favorable for rapid expansion of erythroid progenitors in response to stressful stimuli.[49,50] In the liver, organ IDUA levels increased upon stress, which was also associated with enhanced protein biodistribution into hepatocytes and reduced pathological lesions in all treated mice, including the lowest dose group. Importantly, the therapeutic effects on heart abnormalities, main causes of mortality in patients with Hurler syndrome,[51,52] are also susceptible to transient increases of RBCs and platelets. With 0.1 VCN, heart IDUA levels increased from barely detectable in the unstressed group to 4% of normal, consistent with 2-fold plasma IDUA surge and resulting in complete metabolic correction in the heart. Additional pathologic improvement was observed in the heart of the stressed groups, with as low as 0.005 VCN. Significant and dose-correlated improvement of kidney pathology was found without substantial changes in IDUA or GAG levels in treated mice with >0.03 VCN upon stress, which coincided with more intense $IDUA^+$ signals in glomeruli. Altogether, the data support the notion that concise expansion of transgene-expressing erythroblasts/RBCs and MKs/platelets can enhance therapeutic efficacies in all visceral organs tested, i.e., small changes can make big differences.

The window of boosted efficacy achieved by stimulating the proliferation of reticulocytes and MKs appears to be prolonged, i.e., ~6 weeks after the elevation of IDUA in circulation. The surge of stress-induced plasma IDUA was temporary, peaking on day 7 and declining to baseline levels on day 16 and thereafter. This pattern seems to be closely parallel with the changes of the percentages in reticulocytes and young platelets as well as total platelet counts, although young platelets showed a more rapid response (peaking at day 4). Such short-term elevation of plasma IDUA was most likely due to the enzyme released during an increased MK maturation and RBC/platelet formation in response to blood loss.[19,20] Moreover, the therapeutic benefits persisted for a much longer time, exhibiting continuously reduced GAG accumulation in urine and organs that were associated with additional pathology improvement by the end of the observation period (>day 42). Such sustained benefits may be largely due to the unique delivery routes provided via RBCs and platelets, as described previously. The lifespans of erythrocytes and platelets are 40 days and ~6 days in mice;[53,54] thus, stress-induced therapeutic benefits sustained weeks beyond the elevation of plasma IDUA in mice. Much longer lifespans are expected for human RBCs (up to 120 days)[55] and platelets (~10 days),[56] which would convey more extended, erythroid and EMK-derived therapeutic advantages, i.e., short changes can go a relatively long way.

In clinical HSC transplantation scenarios for the treatment of patients with Hurler syndrome, both cell therapy (mostly via mononuclear cells) and enzyme (in circulation) therapy contribute to the therapeutic effects. We believe that the erythroid and megakaryocytic lineages are one of the main sources for plasma enzyme detected in recipients and play a key role in enzyme distribution in organs. First, the Sly group has shown that human platelets are the richest source of corrective high-uptake (M6P-enriched) beta-glucuronidase (deficient in MPS type VII) among all human tissue or cell types tested.[57–59] Second, we have shown previously that wild-type human promegakaryocytes or murine erythroblasts can release IDUA into the medium during *in vitro* maturation and that WT platelets from MPS/BMT mice contain a significant amount of IDUA, which can be released upon activation.[19,20] Third, using the same EMK lineage-restricted promoter, we have shown previously that intra-platelet IDUA activities in mice with 1% transgene expression were the same as those in WT platelets.[19,20] One may estimate that therapeutic benefits derived from 1% GT in this study setting would be equivalent to enzyme contribution and delivery specifically from EMK lineages after full engraftment of WT HSCs. Based on this estimation, most IDUA enzymes in the circulation of BMT recipients (~80%) are likely derived from EMK lineages of engrafted donor cells.

Gene therapy is becoming a reality worldwide with ~2,600 clinical trials by 2017 and >25% utilizing RV/LV (http://www.abedia.com/wiley/vectors.php). Meanwhile, HSC-mediated gene transfer, with gamma-RV or LV, has been the main gene therapy approach so far in treating LSDs, which are difficult to fully cure due to their involvement in an array of organ systems with a complex set of secondary disease mechanisms. In this proof-of-concept study, we have documented the feasibility of enhancing therapeutic efficacies by promoting erythropoiesis and/or thrombopoiesis in multiple organs of MPS I mice with minimal HSC gene transfer efficiency. Furthermore, preclinical efficacy evaluation with correlation of transgene doses confirms the advantages of using the EMK lineage for highly efficient systemic protein production and release and on-target distribution into monocytes and/or macrophages, which may reduce the burden of high VCNs in HSCs required to achieve clinical benefits. Such advantages can be further augmented by utilizing a hybrid or ubiquitous promoter that can introduce strong expression in monocyte/macrophages, in addition to EMK lineages. The translational application of this concept would be facilitated by utilizing erythropoiesis-stimulating agents, which have been widely used in clinical practice.[60] Moreover, it can take advantage of thrombopoietin receptor-containing proliferation switch that has been reported to stimulate the growth of genetically modified RBCs, platelets, granulocytes, and EMK progenitors (by 2- to 6-fold) in mice,[24] dogs,[25,26] and human $CD34^+$ cells and derivatives,[27,28] in response to the administration of chemical inducers of dimerization (CID, a class of small-molecule drugs). The long-term safety and repeatability of CID-induced temporary proliferation of EMK cells have been indicated in dogs for

up to 9 years.[26] Such a strategy may increase efficacies by selective growth of modified erythroid and MK cells in an inducible, reversible, and repeatable manner. This unique concept may open a door for innovative clinical intervention that may be combined with HSC-based therapy for synergistic treatment of LSDs, especially when large patient-to-patient variations of GT are expected in most clinical trials.

MATERIALS AND METHODS

HSC Gene Transfer and HSC Transplantation

The experimental mice were generated using heterozygous male and females (*Idua*$^{+/-}$) as breeding pairs in a pathogen-free facility (with micro-isolator) at Cincinnati Children's Research Foundation (CCRF) in the vivarium fully accredited by the Association for the Assessment and Accreditation of Laboratory Animal Care (AAALAC). All experimental procedures were performed according to the NIH Guidelines for the Care and Use of Laboratory Animals and were approved by the Institutional Animal Care and Use Committee at CCRF.

Lineage-depleted (Lin$^-$) low-density bone marrow cells (LDBM) were isolated from MPS I mice, transduced with LV at MOI of 40 and transplanted into MPS I mice as previously described.[29] Bone marrow from adult donor mice was isolated for hematopoietic progenitor qualification by hemocytometer cell count. The 8- to 10-week-old *Idua*$^{-/-}$ recipient mice were prepared for transplantation with a lethal dose of irradiation, and they were injected through the tail vein with ~20%, 10%, and 4% donor bone marrow hematopoietic progenitors, respectively, combined with *Idua*$^{-/-}$ progenitors from an adult MPS I donor. Mice injected with 100% WT (*Idua*$^{+/+}$) progenitors are positive controls here.

Blood and Tissue Collection

Blood (20–50 μL) was collected in EDTA from 2 to 5 months after transplantation for assay of IDUA activity in plasma and transduction efficiency monitoring by EGFP FACS analysis. Tissues were collected for biochemical assays after euthanasia. For morphologic studies, each mouse was perfused transcardially through the aorta with cold normal saline briefly. The collected tissue samples were fixed by 4% (w/v) paraformaldehyde fixation or 2% (w/v) glutaraldehyde in 0.175 M sodium cacodylate buffer (pH 7.4) at 4°C.

Immunofluorescent Staining and Flow Cytometry Analysis

Cells from blood were collected in DMEM, centrifuged, suspended in PBS with 0.5% BSA, and stained with PE-conjugated anti-mouse CD41 (BD Biosciences, San Jose, CA) for platelet-specific staining and/or with Thiazole Orange (Sigma-Aldrich) for young platelets and young RBCs. Samples were acquired using a FACS-Calibur (BD Biosciences) flow cytometer. Data were analyzed with FlowJo software (Tree Star, Ashland, OR, USA).

IDUA Enzyme Activity Assay in Plasma and Tissues

The catalytic activity of IDUA was determined using the fluorometric enzyme assays based on the hydrolysis of 4-methylumbelliferone (4-MU)-containing substrates. Cell pellets were homogenized in distilled water using an Ultrasonic Processor (GE-130, Sonics and Materials). Frozen tissue samples were homogenized in lysis buffer (50 mM Tris-HCL, 150 mM NaCl, and 1% Triton) with an Ultrasonic Processor (GE-130, Sonics and Materials). Each incubation comprised 3.5 mM 4-MU-containing fluorogenic substrate and 10 μL cleared lysate, plasma, or tissue supernatant. The fluorescent molecule 4-MU was monitored at 460 nm when excited by 365 nm light against a blank containing the substrate only. Protein concentration was measured by bicinchoninic acid-binding assay (Pierce). The activity was expressed as units per mg of protein. One unit of enzyme activity is defined as the release of 1 nmol 4-MU in a 1-hr reaction at 37°C.

Quantification of Urinary and Tissue GAGs

Urine samples were obtained by bladder palpation. Frozen tissue samples were weighed and placed in K2HPO4 (Sigma, 100 mM) at 200 mg tissue/mL. Samples were homogenized and sonicated for 3 min. The final homogenate was centrifuged at 12,000 × *g*, and supernatants were then treated with proteinase K (Merck; 100 μg/mL final sample concentration) at 56°C overnight. After proteinase K heat inactivation (95°C, 10 min), samples were centrifuged (13,000 × *g*, 20 min) and supernatants were recovered. Then, 10–100 μL proteinase K-digested samples or urine samples were adjusted to 100 μL final volume with K2HPO4 (Sigma, 100 mM). To each sample, 1 mL GAG-complexation 1,9-dimethylmethylene blue (DMMB) solution was added, and samples were vigorously agitated. Then, samples were centrifuged (13,000 × *g*, 10 min) to sediment the solid GAG-DMMB complex, and supernatants were discarded. The GAG-DMMB pellet was then dissolved in 1 mL decomplexation solution by vigorous shaking, and absorbance of the resulting blue solution was measured at 656 nm. A calibration curve, constructed with known amounts of heparin sulfate (Sigma) ranging from 0 to 100 μg/mL, was included in each assay. For each urine sample, creatinine concentration was determined using Creatinine Standard Set (Sigma, C-3613), and GAG values were normalized to creatinine levels as previously described.[29] For a tissue sample, protein concentration was measured by bicinchoninic acid-binding assay (Pierce), and GAG results were expressed in micrograms of GAG per milligram of total protein.

qPCR Analysis

Genomic DNA was isolated from bone marrow with a Gentra Puregene Blood Kit (QIAGEN). The real-time PCR reaction contained 100 ng genomic DNA, 300 nM each of (human) *IDUA*/(mouse) *Apob* primer, and 200 nM TaqMan (human) *IDUA*/(mouse) *Apob* probe. The IDUA primer and probe were designed by Primer Expression 3.0 software, and the sequences were as follows: 5′-CTGGTCTGGTCGGAT GAACA-3′ (FW), 5′-CCGTCCTGAGAGAACTGGATCT-3′ (RW), and 5′-TCCAAGTGCCTGTGGAC-3′ (probe). The cycle of threshold (CT) values of *IDUA* are correlated with *IDUA* transgene copy number to produce the standard curve.

Chemical Staining and Pathology Evaluation

Tissue samples were fixed by 2% (w/v) glutaraldehyde in 0.175 M sodium cacodylate buffer (pH 7.4) at 4°C and sectioned (0.5–1 μm) for light microscopy. Sections were stained with 1% toluidine blue in 1%

sodium borate, followed by examination for the presence of pathological storage vacuoles. Two-four animals per group were analyzed, with over 500 interstitial cells from ~9 sections randomly picked from 2-4 slides. The mean of scoring data from >4 slides is shown for each group.

Immunofluorescent Staining of Tissues

Tissues were removed from animals after perfusion and were post-fixed in 4% paraformaldehyde (PFA). To obtain a frozen section of the liver sample, tissues were incubated overnight at 4°C in 4% PFA containing 30% sucrose. Then, frozen sections (10 μm) were obtained from liver tissues and permeabilized with PBS buffer containing 0.1% Triton X-100. After section permeabilization, PBS buffer containing 5% horse serum and 0.05% Tween-20 was used as blocking solution to block the tissues at room temperature. Sections were then incubated overnight at 4°C with the following primary antibodies: rabbit anti-myc (Invitrogen) to detect the myc-tagged IDUA, rat anti-mouse TER119 (Invitrogen), rat anti-E-cadherin (Invitrogen) and rat anti-CD68 (AbD Serotec, Raleigh, NC) to detect various cell types. Tissue sections were then washed three times with PBS to remove unbound antibodies, followed by incubation with a secondary antibody of the appropriate species (Alexa 488 goat anti-rabbit [Invitrogen] and Alexa 568 goat anti-rat [Invitrogen]). After washing the tissue sections three times with PBS, sections were mounted with Vectashield mounting medium containing DAPI (Vector Laboratories) and analyzed using a DMI6000 B microscope system.

Statistical Analysis

All quantitative assays were performed in duplicate or triplicate from at least 2 experiments. Data are presented as mean ± SD. Statistical analysis was made by either Student's t test or 1-way ANOVA for repeated measurements. p values <0.05 were considered to be statistically significant.

SUPPLEMENTAL INFORMATION

Supplemental Information includes four figures and can be found with this article online at https://doi.org/10.1016/j.omtm.2018.10.001.

AUTHOR CONTRIBUTIONS

Writing – Original Draft, J.H. and D.P.; Methodology, J.H., S.S.E., M.D., and D.P.; Investigation, J.H., S.S.E., M.D., and P.C.; Writing – Review and Editing, J.H., S.S.E., M.D., and D.P.; Conceptualization, D.P.; Supervision, D.P.

CONFLICTS OF INTEREST

The authors have no conflicts of interest.

ACKNOWLEDGMENTS

We are grateful for the technical assistance of Mara Kohls, John Strickley, and the Comprehensive Mouse Core at CCRF. This work was supported by grants from the NIH National Institute of Neurological Disorders and Stroke, United States (NS064330 and NS086134 to D.P.) and Cincinnati Children's Hospital Medical Center (Innovative Pilot Award to D.P.), United States.

REFERENCES

1. Schultz, M.L., Tecedor, L., Chang, M., and Davidson, B.L. (2011). Clarifying lysosomal storage diseases. Trends Neurosci. *34*, 401–410.
2. Platt, F.M. (2018). Emptying the stores: lysosomal diseases and therapeutic strategies. Nat. Rev. Drug Discov. *17*, 133–150.
3. Campos, D., and Monaga, M. (2012). Mucopolysaccharidosis type I: current knowledge on its pathophysiological mechanisms. Metab. Brain Dis. *27*, 121–129.
4. Pan, D. (2011). Cell- and gene-based therapeutic approaches for neurological deficits in mucopolysaccharidoses. Curr. Pharm. Biotechnol. *12*, 884–896.
5. Baum, C., Modlich, U., Göhring, G., and Schlegelberger, B. (2011). Concise review: managing genotoxicity in the therapeutic modification of stem cells. Stem Cells *29*, 1479–1484.
6. Biffi, A. (2017). Hematopoietic Stem Cell Gene Therapy for Storage Disease: Current and New Indications. Mol. Ther. *25*, 1155–1162.
7. Penati, R., Fumagalli, F., Calbi, V., Bernardo, M.E., and Aiuti, A. (2017). Gene therapy for lysosomal storage disorders: recent advances for metachromatic leukodystrophy and mucopolysaccaridosis I. J. Inherit. Metab. Dis. *40*, 543–554.
8. Sessa, M., Lorioli, L., Fumagalli, F., Acquati, S., Redaelli, D., Baldoli, C., Canale, S., Lopez, I.D., Morena, F., Calabria, A., et al. (2016). Lentiviral haemopoietic stem-cell gene therapy in early-onset metachromatic leukodystrophy: an ad-hoc analysis of a non-randomised, open-label, phase 1/2 trial. Lancet *388*, 476–487.
9. Biffi, A., Montini, E., Lorioli, L., Cesani, M., Fumagalli, F., Plati, T., Baldoli, C., Martino, S., Calabria, A., Canale, S., et al. (2013). Lentiviral hematopoietic stem cell gene therapy benefits metachromatic leukodystrophy. Science *341*, 1233158.
10. Williams, D.A. (2013). Broadening the indications for hematopoietic stem cell genetic therapies. Cell Stem Cell *13*, 263–264.
11. Hacein-Bey-Abina, S., Von Kalle, C., Schmidt, M., McCormack, M.P., Wulffraat, N., Leboulch, P., Lim, A., Osborne, C.S., Pawliuk, R., Morillon, E., et al. (2003). LMO2-associated clonal T cell proliferation in two patients after gene therapy for SCID-X1. Science *302*, 415–419.
12. Howe, S.J., Mansour, M.R., Schwarzwaelder, K., Bartholomae, C., Hubank, M., Kempski, H., Brugman, M.H., Pike-Overzet, K., Chatters, S.J., de Ridder, D., et al. (2008). Insertional mutagenesis combined with acquired somatic mutations causes leukemogenesis following gene therapy of SCID-X1 patients. J. Clin. Invest. *118*, 3143–3150.
13. Rivière, I., Dunbar, C.E., and Sadelain, M. (2012). Hematopoietic stem cell engineering at a crossroads. Blood *119*, 1107–1116.
14. Kohlscheen, S., Bonig, H., and Modlich, U. (2017). Promises and Challenges in Hematopoietic Stem Cell Gene Therapy. Hum. Gene Ther. *28*, 782–799.
15. Blair, P., and Flaumenhaft, R. (2009). Platelet alpha-granules: basic biology and clinical correlates. Blood Rev. *23*, 177–189.
16. Kaushansky, K. (2005). The molecular mechanisms that control thrombopoiesis. J. Clin. Invest. *115*, 3339–3347.
17. Shi, Q., Fahs, S.A., Kuether, E.L., Cooley, B.C., Weiler, H., and Montgomery, R.R. (2010). Targeting FVIII expression to endothelial cells regenerates a releasable pool of FVIII and restores hemostasis in a mouse model of hemophilia A. Blood *116*, 3049–3057.
18. Cox, T.M., and Cachón-González, M.B. (2012). The cellular pathology of lysosomal diseases. J. Pathol. *226*, 241–254.
19. Wang, D., Zhang, W., Kalfa, T.A., Grabowski, G., Davies, S., Malik, P., and Pan, D. (2009). Reprogramming erythroid cells for lysosomal enzyme production leads to visceral and CNS cross-correction in mice with Hurler syndrome. Proc. Natl. Acad. Sci. USA *106*, 19958–19963.
20. Dai, M., Han, J., El-Amouri, S.S., Brady, R.O., and Pan, D. (2014). Platelets are efficient and protective depots for storage, distribution, and delivery of lysosomal enzyme in mice with Hurler syndrome. Proc. Natl. Acad. Sci. USA *111*, 2680–2685.
21. Biffi, A., Aubourg, P., and Cartier, N. (2011). Gene therapy for leukodystrophies. Hum. Mol. Genet. *20* (R1), R42–R53.
22. Cavazzana-Calvo, M., Dal-Cortivo, L., André-Schmutz, I., Hacein-Bey Abina, S., and Fischer, A. (2007). [Cell therapy for inherited diseases of the hematopoietic system]. C. R. Biol. *330*, 538–542.

23. Zhao, J., Edgren, G., and Stanworth, S.J. (2017). Is there a standard-of-care for transfusion support of patients with haematological malignancies? Curr. Opin. Hematol. *24*, 515–520.

24. Jin, L., Zeng, H., Chien, S., Otto, K.G., Richard, R.E., Emery, D.W., and Blau, C.A. (2000). In vivo selection using a cell-growth switch. Nat. Genet. *26*, 64–66.

25. Neff, T., Horn, P.A., Valli, V.E., Gown, A.M., Wardwell, S., Wood, B.L., von Kalle, C., Schmidt, M., Peterson, L.J., Morris, J.C., et al. (2002). Pharmacologically regulated in vivo selection in a large animal. Blood *100*, 2026–2031.

26. Okazuka, K., Beard, B.C., Emery, D.W., Schwarzwaelder, K., Spector, M.R., Sale, G.E., von Kalle, C., Torok-Storb, B., Kiem, H.P., and Blau, C.A. (2011). Long-term regulation of genetically modified primary hematopoietic cells in dogs. Mol. Ther. *19*, 1287–1294.

27. Nagasawa, Y., Wood, B.L., Wang, L., Lintmaer, I., Guo, W., Papayannopoulou, T., Harkey, M.A., Nourigat, C., and Blau, C.A. (2006). Anatomical compartments modify the response of human hematopoietic cells to a mitogenic signal. Stem Cells *24*, 908–917.

28. Belay, E., Miller, C.P., Kortum, A.N., Torok-Storb, B., Blau, C.A., and Emery, D.W. (2015). A hyperactive Mpl-based cell growth switch drives macrophage-associated erythropoiesis through an erythroid-megakaryocytic precursor. Blood *125*, 1025–1033.

29. El-Amouri, S.S., Dai, M., Han, J.F., Brady, R.O., and Pan, D. (2014). Normalization and improvement of CNS deficits in mice with Hurler syndrome after long-term peripheral delivery of BBB-targeted iduronidase. Mol. Ther. *22*, 2028–2037.

30. Dobbelstein, M. (2003). Viruses in therapy–royal road or dead end? Virus Res. *92*, 219–221.

31. Thomas, C.E., Ehrhardt, A., and Kay, M.A. (2003). Progress and problems with the use of viral vectors for gene therapy. Nat. Rev. Genet. *4*, 346–358.

32. Omokawa, S., Notoya, T., Kumagai, M., Takada, G., Watanabe, E., Echigoya, Y., Saito, M., Abe, M., Osato, N., and Kawakami, K. (2001). Status of platelet collection and platelet transfusion. Ther. Apher. *5*, 17–21.

33. Kaushansky, K. (2008). Cell expansion and maintenance of stemness. Blood *111*, 3920–3921.

34. Geddis, A.E., and Kaushansky, K. (2007). Immunology. The root of platelet production. Science *317*, 1689–1691.

35. Tarantal, A.F., McDonald, R.J., Jimenez, D.F., Lee, C.C., O'Shea, C.E., Leapley, A.C., Won, R.H., Plopper, C.G., Lutzko, C., and Kohn, D.B. (2005). Intrapulmonary and intramyocardial gene transfer in rhesus monkeys (Macaca mulatta): safety and efficiency of HIV-1-derived lentiviral vectors for fetal gene delivery. Mol. Ther. *12*, 87–98.

36. Lizzi Lagranha, V., Zambiasi Martinelli, B., Baldo, G., Ávila Testa, G., Giacomet de Carvalho, T., Giugliani, R., and Matte, U. (2017). Subcutaneous implantation of microencapsulated cells overexpressing α-L-iduronidase for mucopolysaccharidosis type I treatment. J. Mater. Sci. Mater. Med. *28*, 43.

37. Hacein-Bey Abina, S., Gaspar, H.B., Blondeau, J., Caccavelli, L., Charrier, S., Buckland, K., Picard, C., Six, E., Himoudi, N., Gilmour, K., et al. (2015). Outcomes following gene therapy in patients with severe Wiskott-Aldrich syndrome. JAMA *313*, 1550–1563.

38. Aiuti, A., Biasco, L., Scaramuzza, S., Ferrua, F., Cicalese, M.P., Baricordi, C., Dionisio, F., Calabria, A., Giannelli, S., Castiello, M.C., et al. (2013). Lentiviral hematopoietic stem cell gene therapy in patients with Wiskott-Aldrich syndrome. Science *341*, 1233151.

39. De Ravin, S.S., Wu, X., Moir, S., Anaya-O'Brien, S., Kwatemaa, N., Littel, P., Theobald, N., Choi, U., Su, L., Marquesen, M., et al. (2016). Lentiviral hematopoietic stem cell gene therapy for X-linked severe combined immunodeficiency. Sci. Transl. Med. *8*, 335ra57.

40. Ribeil, J.A., Hacein-Bey-Abina, S., Payen, E., Magnani, A., Semeraro, M., Magrin, E., Caccavelli, L., Neven, B., Bourget, P., El Nemer, W., et al. (2017). Gene Therapy in a Patient with Sickle Cell Disease. N. Engl. J. Med. *376*, 848–855.

41. Cartier, N., Hacein-Bey-Abina, S., Bartholomae, C.C., Veres, G., Schmidt, M., Kutschera, I., Vidaud, M., Abel, U., Dal-Cortivo, L., Caccavelli, L., et al. (2009). Hematopoietic stem cell gene therapy with a lentiviral vector in X-linked adrenoleukodystrophy. Science *326*, 818–823.

42. Visigalli, I., Delai, S., Politi, L.S., Di Domenico, C., Cerri, F., Mrak, E., D'Isa, R., Ungaro, D., Stok, M., Sanvito, F., et al. (2010). Gene therapy augments the efficacy of hematopoietic cell transplantation and fully corrects mucopolysaccharidosis type I phenotype in the mouse model. Blood *116*, 5130–5139.

43. Soper, B.W., Duffy, T.M., Vogler, C.A., and Barker, J.E. (1999). A genetically myeloablated MPS VII model detects the expansion and curative properties of as few as 100 enriched murine stem cells. Exp. Hematol. *27*, 1691–1704.

44. Ou, L., Herzog, T., Koniar, B.L., Gunther, R., and Whitley, C.B. (2014). High-dose enzyme replacement therapy in murine Hurler syndrome. Mol. Genet. Metab. *111*, 116–122.

45. Lutzko, C., Kruth, S., Abrams-Ogg, A.C., Lau, K., Li, L., Clark, B.R., Ruedy, C., Nanji, S., Foster, R., Kohn, D., et al. (1999). Genetically corrected autologous stem cells engraft, but host immune responses limit their utility in canine alpha-L-iduronidase deficiency. Blood *93*, 1895–1905.

46. Liu, C., Dunigan, J.T., Watkins, S.C., Bahnson, A.B., and Barranger, J.A. (1998). Long-term expression, systemic delivery, and macrophage uptake of recombinant human glucocerebrosidase in mice transplanted with genetically modified primary myoblasts. Hum. Gene Ther. *9*, 2375–2384.

47. Sands, M.S., and Davidson, B.L. (2006). Gene therapy for lysosomal storage diseases. Mol. Ther. *13*, 839–849.

48. Kaushansky, K. (2009). Determinants of platelet number and regulation of thrombopoiesis. Hematology Am. Soc. Hematol. Educ. Program *2009*, 147–152.

49. Lenox, L.E., Perry, J.M., and Paulson, R.F. (2005). BMP4 and Madh5 regulate the erythroid response to acute anemia. Blood *105*, 2741–2748.

50. Harandi, O.F., Hedge, S., Wu, D.C., McKeone, D., and Paulson, R.F. (2010). Murine erythroid short-term radioprotection requires a BMP4-dependent, self-renewing population of stress erythroid progenitors. J. Clin. Invest. *120*, 4507–4519.

51. Parini, R., Deodato, F., Di Rocco, M., Lanino, E., Locatelli, F., Messina, C., Rovelli, A., and Scarpa, M. (2017). Open issues in Mucopolysaccharidosis type I-Hurler. Orphanet J. Rare Dis. *12*, 112.

52. Aldenhoven, M., Jones, S.A., Bonney, D., Borrill, R.E., Coussons, M., Mercer, J., Bierings, M.B., Versluys, B., van Hasselt, P.M., Wijburg, F.A., et al. (2015). Hematopoietic cell transplantation for mucopolysaccharidosis patients is safe and effective: results after implementation of international guidelines. Biol. Blood Marrow Transplant. *21*, 1106–1109.

53. Van Putten, L.M. (1958). The life span of red cells in the rat and the mouse as determined by labeling with DFP32 in vivo. Blood *13*, 789–794.

54. Mason, K.D., Carpinelli, M.R., Fletcher, J.I., Collinge, J.E., Hilton, A.A., Ellis, S., Kelly, P.N., Ekert, P.G., Metcalf, D., Roberts, A.W., et al. (2007). Programmed anuclear cell death delimits platelet life span. Cell *128*, 1173–1186.

55. Leeksma, C.H., and Cohen, J.A. (1955). Determination of the life of human blood platelets using labelled diisopropylfluorophosphanate. Nature *175*, 552–553.

56. Daly, M.E. (2011). Determinants of platelet count in humans. Haematologica *96*, 10–13.

57. Brot, F.E., Glaser, J.H., Roozen, K.J., Sly, W.S., and Stahl, P.D. (1974). In vitro correction of deficient human fibroblasts by beta-glucuronidase from different human sources. Biochem. Biophys. Res. Commun. *57*, 1–8.

58. Kaplan, A., Achord, D.T., and Sly, W.S. (1977). Phosphohexosyl components of a lysosomal enzyme are recognized by pinocytosis receptors on human fibroblasts. Proc. Natl. Acad. Sci. USA *74*, 2026–2030.

59. Natowicz, M.R., Chi, M.M., Lowry, O.H., and Sly, W.S. (1979). Enzymatic identification of mannose 6-phosphate on the recognition marker for receptor-mediated pinocytosis of beta-glucuronidase by human fibroblasts. Proc. Natl. Acad. Sci. USA *76*, 4322–4326.

60. Rohner, E., Grabik, M., Tonia, T., Jüni, P., Pétavy, F., Pignatti, F., and Bohlius, J. (2017). Does access to clinical study reports from the European Medicines Agency reduce reporting biases? A systematic review and meta-analysis of randomized controlled trials on the effect of erythropoiesis-stimulating agents in cancer patients. PLoS ONE *12*, e0189309.